Vol.2,No.1,2
Winter&Spring,1991

ANALYSIS OF SOME MAGNETIC PROPERTIES OF DILUTED MAGNETIC SEMICONDUCTORS

H. Akbarzadeh

Department of Physics , Isfahan University of Technology , Isfahan, Islamic Republic of Iran

Abstract

The susceptibility and specific heat experimental results of the diluted magnetic semiconductors (DMS) are incorporated in a model based on short-range as well as long-range interaction in a random array of magnetic ions. The so-called nearest-neighbor pair approximation (NNPA) is applied. It appears that the calculated values of zero field specific heat and Curie-Weiss temperature based on the model calculation are in good agreement with experimental results.

Introduction

Diluted Magnetic Semiconductors (DMS) [1] also referred to as Semimagnetic Semiconductors (SMSC) [2] belong to a novel class of materials which have been intensively studied by various methods during recent years because of their important semiconducting as well as magnetic properties [3].

DMS are in fact solid solutions of the $A_{1-x}M_xB$ type which are formed by substitution of the A component in an ordinary semiconductor AB of the II-V or II-VI group by a magnetic 3d or 4f M component. As the MB compound is a magnetic and AB is a normal, non-magnetic semiconductor then $A_{1-x}M_xB$ is the link between them and the terminology "Semimagnetic Semiconductors" reflects the situation. On the other hand, diluting magnetic compounds MB with non-magnetic A ions we can refer to $A_{1-x}M_xB$ compounds as "Diluted Magnetic Semiconductors".

The most extensively studied materials of this type are the $A^{II}_{1-X}Mn_XB^{VI}$ alloys in which a fraction of the group II Sublattice is replaced at random by Mn.

Keywords: Spin Glass, Diluted Magnetic Semiconductors (DMS), Semimagnetic Semicondutors

A=Zn, Cd, Hg are group II elements of the periodic table, B=S, Se, Te are group VI elements and x is the mole fraction of the magnetic Mn^{2+}.

Diluted Magnetic Semiconductors are of interest for several reasons:

First, their semiconducting properties (in zero magnetic field) such as the lattice constant, the band gap, the effective mass, etc. can be varied in a controlled fashion by varying the composition of the material, similar to non-magnetic three element compounds such as $Hg_{1-x}Cd_xTe$, $Pb_{1-x}Sn_xTe$, etc. This tunability of the energy gap by composition makes DMS compounds excellent candidates for infra-red detector application as well as for the preparation of quantum well and super lattices [3].

Secondly, one of the most interesting differences between magnetic compounds ($A_{1-x}Mn_xB$) with non-magnetic host (AB) arises from the exchange interaction of the S and P band electrons of the DMS and the 3d [5] electrons associated with the Mn^{++} ions. It is because of this sp-d exchange interaction that wide gap DMS such as $Cd_{1-x}Mn_xTe$ or $Cd_{1-x}Mn_xSe$ exhibit giant Faraday rotation (of the order of 1000 ^{0}/cm kG) at liquid

helium temperatures [4]. The large size of Faraday rotation offers some optical Device applications such as Isolators, Circulators, Modulators, etc. Furthermore, the large size of the effect can be exploited in highly sensitive magnetometers, for measuring static as well as dynamic magnetic fields (up to GHz frequencies). Also, the observation of stimulated spin-flip Raman scattering in n-type $Hg_{1-x}Mn_xTe$ suggests the possibility of using narrow gap DMS for the construction of a stimulated spin-flip Raman laser which is tunable over a wide range [5].

Thirdly, the random distribution of magnetic ions over the cation sublattice leads to important magnetic effects, e.g., the formation of the spin-glass phase at low temperature.

Originally the spin-glass transition was interpreted as arising from interactions between Mn ions situated at the nearest-neighbor (nn) sites in the host lattice [6,7] This conjecture was supported by the original observation of the spin-glass transition only for Mn concentrations above the percolation limit (x>0.18) [8]. It was suggested then that the spin-glass transition was brought about by frustration caused by the short-range antiferromagnetic interaction between nearest manganese neighbors on the high symmetry host lattice. Recent results, however, for low Mn concentrations in $Hg_{1-x}Mn_xTe$, $(Cd_{1-x}Mn_x)_3As_2$, $(Zn_{1-x}Mn_x)_3As_2$, $Cd_{1-x}Mn_xTe$, $Cd_{1-x}Mn_xSe$, $Zn_{1-}Mn_xTe$ and $Zn_{1-x}Mn_xSe$, reveal the existence of a spin-glass phase also below the percolation limit (x<xc) [8,9,10] These facts invalidate the arguments related to the mechanism of spin-glass formation in these materials as given before.

Moreover, in the interpretation of the experimental data in terms of various existing models no consistent set of interaction parameters explaining all the magnetic data simultaneously has been obtained. It seems that this discrepancy is mainly due to the fact that the long-range interaction is not taken into account in these oversimplified models. This underestimating gives rise to a wide spread of exchange parameters obtained from various experimental data and the questionable need to adjust the statistical distribution of the magnetic ions [11]. However, an effort to reconcile these contradictory viewpoints has not yet been undertaken.

In an attempt to interpret the susceptibility and specific heat experimental results simultaneously on the basis of a unique model we decided to study the magnetic properties of DMS compounds in some detail.

We reanalyzed the published data (as well as some unpublished results) by applying a recently proposed model based on incorporating nearest-neighbor exchange interaction (J_1) as well as long-range interaction of the type J/(R)n between magnetic ions in a random statistical distribution.

Discussion

Originally, the magnetic behavior of diluted magnetic semiconductors was more or less interpreted based on the following considerations:

(i) a cluster model based on the nearest-neighbor interaction was applied. (The interaction beyond nearest-neighbor was ignored)

(ii) The spin-glass behavior ascribed to the frustration of the antiferromagnetic interactions inherent in an fcc sublattice over which the Mn ions are distributed.

Based on these assumptions the spin-glass transition was expected only above the percolation limit (xc) of the host lattice. At that time spin-glass phase was only observed for samples with concentrations above the percolation limit, and this led to the conclusion that the long-range interactions were really ignorable.

Additionally, in order to obtain agreement between calculated and cxperimental results, it was assumed that the distribution of Mn ions deviates strongly from a random distribution [11]. Subsequent calculations on the basis of nearest-neighbor interactions only gave rise to a widespread of exchange parameters deduced from various sets of data.

Nagata et al. [11], for example, in a systematic magnetic study of $Hg_{1-x}Mn_xTe$ found the nearest-neighbor exchange constant J/kB to be about- 0.7 ± 0.3K which is substantially smaller than that obtained by previous workers [12]. They also had to adjust the random distribution of the magnetic ions, e.g. the number of single ions had to be reduced by about 30% of the number corresponding to a purely random distribution [11].

Recently, new information became available on the behavior of Mn ions in the diluted magnetic semiconductors that invalidates the above arguments.

Firstly, extension of the experimental results for low Mn concentrations reveals the existence of spin-glass

phase also for Mn concentrations below the percolation limit [13].

Secondly, high field magnetization measurements show that the nearest-neighbor Heisenberg interaction energy J/kB is of the order of 10K [14,15], substantially higher than that expected by Nagata et al .[11].

It is claimed that these discrepancies are mainly due to the fact that the long-range character of the interactions are not taken into account [16]. We, therefore, will try to interpret the susceptibility and specific heat results simultaneously on the basis of one model incorporating short-range as well as long-range interactions in a random array.

We apply the so-called Nearest-Neighbor Pair-Approximation model (NNPA). It has been introduced by Matho [17] for canonical metallic spin-glasses and was recently successfully used for DMS's as well [9,10]. It is based on the assumption that the partition function of a random macroscopic system with a long-range interaction may be factorized into contributions of pairs. In this case, each spin is considered to be coupled by an exchange interaction J only to its nearest magnetic neighbor which may be located anywhere at a distance R from the reference site.

Table I

Numberof υ^{th} neighbors, N_υ and distances to them in units R_1

fcc		(hcp)	
$(R_\upsilon)^2/(R_1)^2$	N_υ	$(R_\upsilon)^2/(R_1)^2$	N_υ
1	12	1	12
2	6	2	6
3	24	3	2
4	12	4	18
5	24	5	12
6	8	6	6
7	48	7	12
8	6	8	12
9	36	9	6
10	24	10	6
11	24	11	12
12	24	12	24
13	72	13	6
14	48	14	12
15	12	15	12
16	48	16	24
17	30	17	12
18	72	18	12
19	24	19	2

The lattice sites of the crystalline host structure are arranged in shells at distances (R_υ, υ = 1,2, 3,..) around the reference site; the υ^{th} shell contains N_υ lattice sites. Table I shows the number of lattice sites, N_υ, in each shell. (R_υ is expressed in units of the nearest-neighbor distance, R_1= 1). In Figure 1 a schematic picture of the lattice sites distribution for fcc crystal is shown in two dimensions. The circles are the projection of shells with radius R_υ ($R_1 = a\sqrt{2/2}$, $R_2 = \sqrt{2}\,R_1 = a$,

$R_3 = \sqrt{3}\,R_1 = \sqrt{\frac{6}{2}}\,a$, $R_4 = 2R_1 = a\sqrt{2}$, a =lattice parameter)

in a cube face. The radius of the first two circles are the same as the related shells radiuses but generally they are different. Let's assume that the reference site is occupied by a magnetic ion. Considering that the magnetic ions are distributed randomly throughout the lattice, then the probability of finding the nearest magnetic ion in the υ^{th} shell is elaborated as follows:

As x= The mole fraction of the magnetic ion, then: x= The probability for a specific site to be occupied by a magnetic ion.

1-x = The probability for a specific site to be occupied by a non-magnetic ion.

$(1-x)^{N_\upsilon}$ = The probability for υ^{th} shell to be totally occupied by non-magnetic ions

$(1-x)^{N_1}(1-x)^{N_2}\ldots(1-x)^{N_{\upsilon-1}}$ = The probability for all shells with $\upsilon^1 < \upsilon$ totally occupied by non-magnetic ions $1-(1-x)^{N_\upsilon}$ =The probability for υ^{th} shell not to be totally occupied by non-magnetic ions (at least one magnetic ion is located in υ^{th} shell).

Now , if we define:

$p_\upsilon(x)$ = The probability of finding the nearest magnetic ion in the υ^{th} shell (assuming all $\upsilon^1 < \upsilon$ shells empty) then;

$$P_\upsilon(x) = \left[(1-x)^{N_1}(1-x)^{N_2}\ldots(1-x)^{N_{\upsilon-1}}\right]\left[1-(1-x)^{N_\upsilon}\right]P_\upsilon(x)$$

is a product of: (a) The probability for a magnetic ion to have a magnetic neighbor at a distance R_υ , and (b) The probability that both magnetic ions do not belong to a pair with a shorter R_υ

We then obtain:

$$P_v(x)=\left[(1-x)^{N_1}(1-x)^{N_2}....(1-x)^{N_{v-1}}\right]\left[1-(1-x)^{N_v}\right] \quad (1)$$

$$P_v(x)=\left[(1-x)^{N_1+N_2+.....N_{v-1}}\right]\left[1-(1-x)^{N_v}\right] \quad (2)$$

Using $n_v=\sum_{v=1}^{v} N_v$ for $v>o$, $n_0=0$

$$P_v(x)=(1-x)^{n_{v-1}}\left[1-(1-x)^{N_v}\right] \quad (3)$$

$$P_v(x)=(1-x)^{n_{v-1}}-(1-x)^{n_v} \quad (4)$$

The total partition function and other thermodynamic functions like the specific heat, magnetization, and susceptiblity can be calculated by summing the respective pair contributions:

$$Z=\sum_{V=1}^{\infty} Z_V P_V(x)/2 \quad (5)$$

$$C_m=\sum_{V=1}^{\infty} C_{mV} P_V(x)/2 \quad (6)$$

The summation over the shells (v) is carried out up to shell $v=\bar{v}$ for which $\sum_{V=1}^{\bar{v}} P_V(x)\geq 0.99$. The value of $\bar{v}$ was taken as 19 for low concentrations ($x<0.03$). For higher concentrations a smaller $\bar{v}$ was sufficient. Each pair contribution (C_m,v) contains the exchange parameter J_V. The Hamiltonian for a pair is given by:

$$H_V^P=-2J_V\vec{S_i}..\vec{S_V}-g\mu_B(S_i^z+S_V^z)B^z \quad (7)$$

Where $J_V=J(R_V)$ and R_V denotes the distance between the sites i and v. Considering S1 = S2 = 5/2, g=2 and $\vec{S1}+\vec{S2}=\vec{S}$ then Hamiltonian eigenvalue for pair clusters can be obtained as follows:

$$2\vec{S_1}.\vec{S_2}=(\vec{S_1}+\vec{S_2})^2-(\vec{S_1})^2-(\vec{S_2})^2 \quad (8)$$

Then

Then $H\psi=-2J(\vec{S_1}.\vec{S_2})\psi-g\mu_B B(S_1^z+S_2^z)\psi=$

$$-J\left[S(S+1)-S_1(S_1+1)-S_2(S_2+1)\right]\psi-\Psi-g\mu_B Bm\Psi \quad (9)$$

$$E=-J[S(S+1)-35/2]-g\mu_B Bm \quad (10)$$

$0\leq S\leq 5$, $|m|\leq 5$

The zero field energy levels of the pair is shown in Fig. 2.

The specific heat for each pair is given by:

$$C_{m,v}=\frac{\partial}{\partial T}\left[\frac{\sum_{S=0}^{5} E_S \exp(-Es/k_BT)}{\sum_{S=0}^{5} exp(-Es/k_BT)}\right] \quad (11)$$

In the presence of a magnetic field, E_S is changed to $E_S-g\mu_B mB$ where m is the magnetic quantum number.

To calculate the magnetic specific heat the radial dependence of the exchange interaction, $J_V=J(R_V)$, should be given by experimental data. This procedure is elaborated as follows:

It is well known that a spin glass freezes when the thermal energy k_BT is comparable to the average magnetic interaction energy $\bar{E}$. It is furthermore assumed that $\bar{E}$ is proportional to J (R) where J(Rij) is the exchange constant describing the interaction between two magnetic ions separated by Rij and R is the mean magnetic distance.

Additionally using the scaling analysis for a random distribution it is assumed that $R^3x=$ const.. For a particular powerlike or exponential R- dependence of the freezing temperature, T_f, can be derived as:

$$\bar{E}=J(R)S^2\approx k_BT_f \quad (12)$$

$$\text{FOR } J(R)\alpha e^{-\alpha R}\Rightarrow \bar{E}\alpha e^{-\alpha R} \quad (13)$$

$$\text{Then } T_f\alpha e^{-\alpha R}\Rightarrow \ln T_f\alpha(-\alpha R) \quad (14)$$

$$\text{As } R^3x=\text{const.}\Rightarrow \ln T_f\alpha(-\alpha x^{-1/3}) \quad (15)$$

$$\text{FOR } J(R)\alpha R^{-n}\Rightarrow \ln T_f\alpha(-n\ln R) \quad (16)$$

$$\text{As } 3\ln R+\ln x=\text{const.} \quad (17)$$

$$\text{Then } \ln T_f\alpha\frac{n}{3}\ln x \quad (18)$$

A comparison between the experimental data and these calculations shows that the power law yields a better fit than an exponential decay from far below to far above the percolation limit [16]. Then exponent n

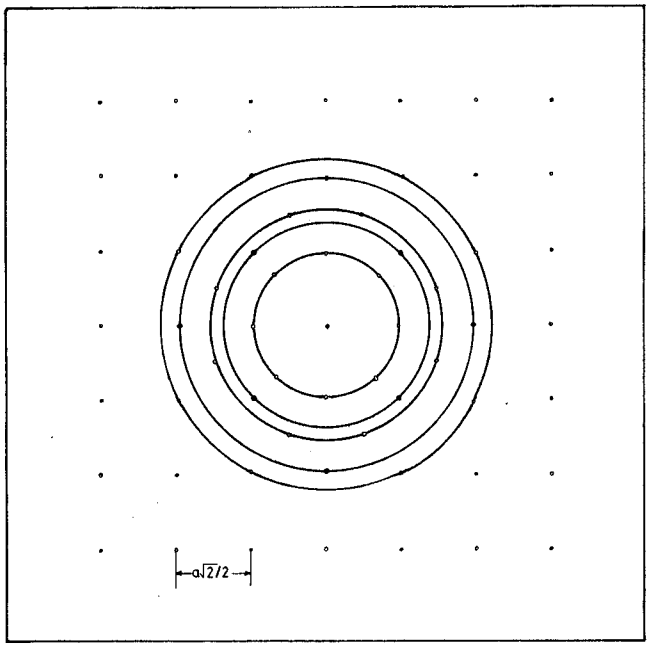

Fig.1. Schematic picture of the host sites distribution for fcc crystal in two dimensions. (.) Indicates the lattice points at the corners while (o) indicates the lattice points at the face centers.

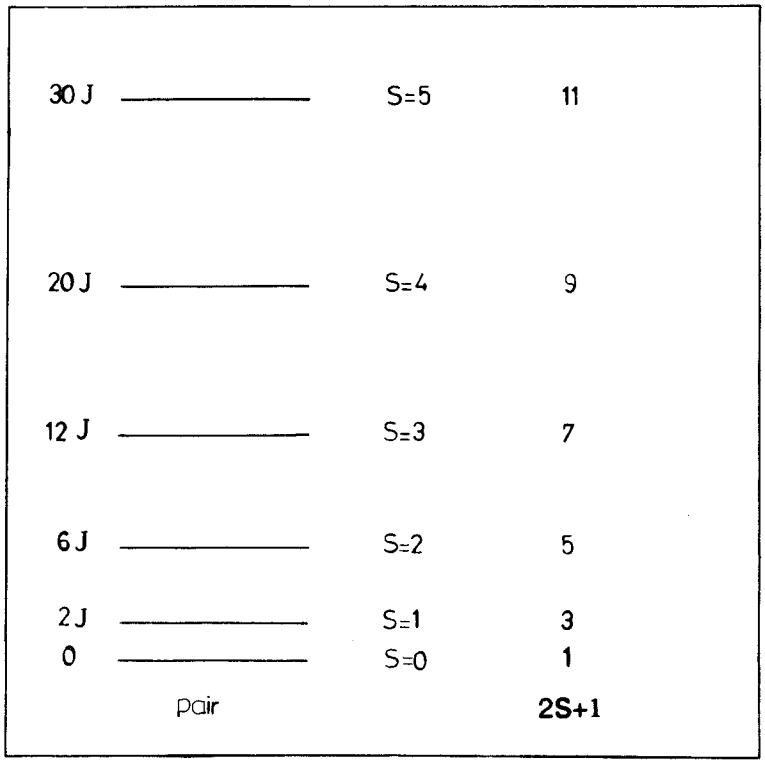

Fig.2. Energy levels for a pair. The values of the degeneracy (2_s+1) are indicated.

deduced from experimental results are shown in Table II, following Ref. 16.

Table II

The exponent n value deduced from experimental data

Material	X-range	n
Zn_1-xMn xSe	0.3 - 0.4	6.8
Hg_1-xMn xSe	0.02 - 0.3	5.0

It is relevant to note that some workers claim that for open gap DMS (Cd_1 - $_x$Mn $_x$ Te/Se) the T_f -x diagrams are in agreement with the exponential decay, consistent with the Bloembergen-Rowland prediction [18].

We would also like to stress here that experimental data shows no concentration dependence of nearest-neighbor exchange interaction (J_{nn}) [14], whereas spin-glass freezing temperature T_f depends on concentration. It can be an indication that in spin-glass creation only the long-range part of exchange interaction is important. We therefore suggest a qualitative model which gives some insight into the magnetic properties of Diluted Magnetic Semiconductors:

At high temperatures, $T>>T_f$, the system is Parramagnetic. At $T>T_f$ small clusters are created and all nearest-neighbor Mn ions are in clusters. At $T\sim T_f$ spin-glass will happen in the nearest-neighbor ions which do not have any considerable effect and the interaction for the next nearest-neighbor or higher will have an effect on T_f. Indeed long-range exchange interaction will connect the small clusters for block formation and short-range interaction (nearest-neighbor) has no considerable effect on big cluster formation. Figure 3 shows a schematic picture of spin-glass formation.

Interpretation

In order to interpret the susceptibility and specific heat data simultaneously on the basis of one model incorporating a nearest-neighbor as well as a long-range interaction in a random array, we stress the following assumptions:

(i) An antiferromagnetic (AF) nearest and next nearest-neighbor interactions J_1 and J_2 experimental measurements of magnetic susceptiblity, indicate that at high temperatures it displays a Curie-Weiss behavior with negative Curie-Weiss temperature, indicating antiferromagnetic interactions between the spins. (ii) An AF long-range interaction of the type $J/(R)^n$ for ions beyond next nearest-neighbor where n is 6.8 for open

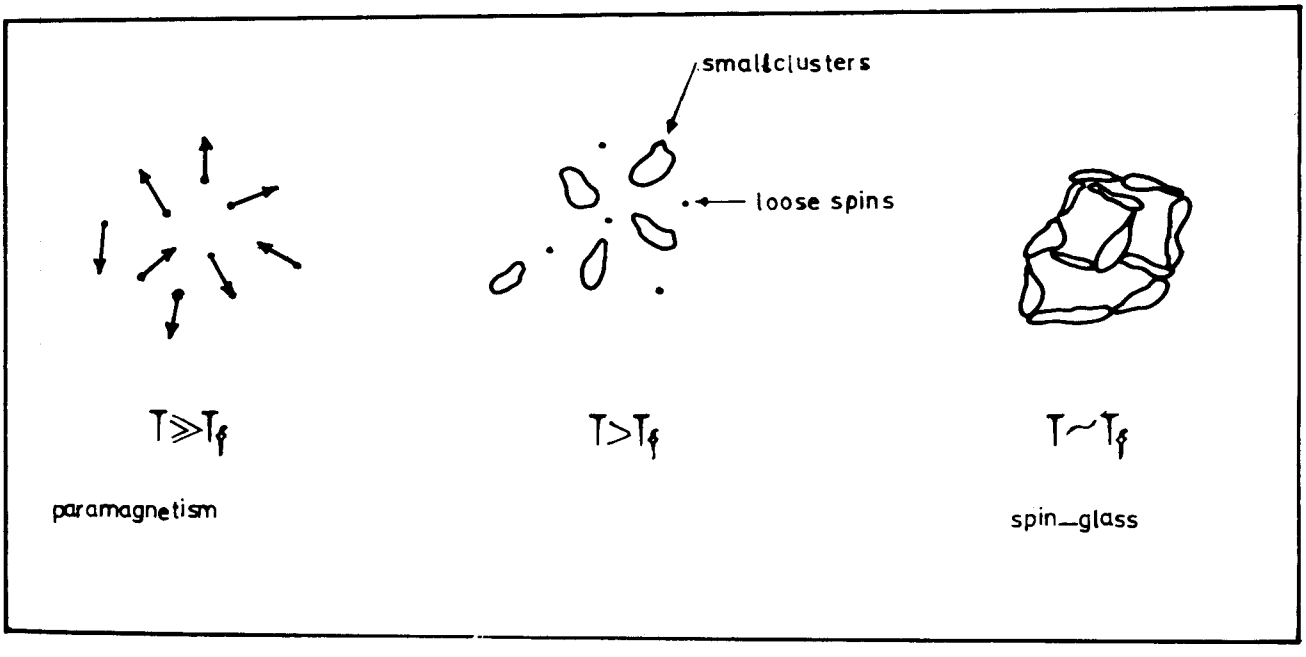

Fig.3. Schematic picture of spin-glass formation.

gap and 5 for zero gap DMS's.

(iii) A random distribution of Mn ions (in contrast to Nagata et al. [11] assumption). Spalek et al. [19] analytically derived the static magnetic susceptibility based on random distribution and showed that in the high temperature limit they obey the Curie-Weiss law. (iv) g = 2, S = 5/2, based on susceptibility results [19,20] (in contrast to Oseroff results [21])

This model is similar to the model used for the interpretation of the results on $(Cd_{1-x}Mn_x)_3As_2$ [8] and $(Zn_{1-x}Mn_x)_3As_2$ [8] Nearest-neighbor interaction J_1 is chosen as a constant value, but J_2 and J are treated as adjustable parameters. Relatively accurate values of J_1 are given in Table III. With these parameters we calculated C_m with the NNPA method for $Zn_{1-x}Mn_xSe$ (x = 0.01) and compared them with the experimental data. The results are shown in Fig. 4. It is seen that, on the whole, the agreement between calculated results, and the experimental data is fair.

Additionally we would like to make the following comments;

As in-zero magnetic field single Mn ions will not contribute to specific heat at low temperatures, then the concentration of active magnetic ions contributing to the specific heat is lower than nominal value.

Keesom [22] by measuring the low temperature specific heat of the same sample obtained x = O.OO81 as the minimum active concentration which is in excellent agreement with our calculated results. Furthermore, the value of next nearest-neighbor integral J_2 obtained by calculation is comparable with the results of other workers [20, 22].

Hereafter we apply the model to obtain the value of the Curie-Weiss temperature. As shown by Spalek et al. [19] the calculation of magnetic susceptibility in the high temperature limit yields the Curie-Weiss behavior;

$$\chi = \frac{C(x)}{T-\theta(x)} \qquad (19)$$

The Curie-Weiss temperature $\theta(x)$ is given by;

$$\theta(x) = \left[2/3\, S(S+1) \sum_v J_v N_v / k_B\right] x = \theta_0 x \qquad (20)$$

Where J_v is the exchange integral between neighbors and N_v is the number of cations in the coordination sphere around a given cation chosen as the central one. If the localized magnetic moments are subjected to a nearest-neighbor exchange J_1 a next nearest-neighbor exchange J_2 supplemented with a long-range interaction of the type $J(R) = JR^{-n}$ for further neighbors, yields

$$\theta(x) = \frac{2S(S+1)x}{3k_B}\left[N_1 J_1 + N_2 J_2 + \sum_{j=3}^{\infty} N_j J R_j^{-n}\right] \qquad (21)$$

Where R_j is in units of the nearest-neighbor distance, $R_1 = 1$.

N_V as the number of neighbors at distance R_V (R_V expressed in units of the nearest-neighbor Mn distance) are given in Table I.

It is known that the crystal structure of nearly all $A^{II}1-_xMn_xB^{VI}$ alloys is zinc blende (except CdMnS/Se). So, hereafter calculations are confined to this structure. Then for wide gap DMS we have

$$\theta(x) = \frac{35X}{6kB}\left[12 J_1 + 6 J_2 + J\left(\frac{24}{(\sqrt{3})^{6.8}} + \frac{12}{(\sqrt{4})^{6.8}} + \ldots\right)\right] \qquad (22)$$

Then;

$$\theta(x) = \frac{35\,x}{6kB}\left[12 J_1 + 6 J_2 + 13.7 J\right] \qquad (23)$$

Substitution of J_1, J_2 and J value for $Zn_1 - _xMn_xSe$ (x = 0.01) in the preceding expression results in θ_0 = 948 K

Furdyna et al. [20] investigating the static magnetic susceptibility of $Z_{n1} - _xMn_xSe$, yields θ_0=944 K which is in excellent agreement with our results.

We extended similar investigation to $Hg_1 - _xMn_xSe$ (x= 0.01). The results are shown in Fig.5. In $Hg_1 - _xMn_xSe$ (x = 0.01) for best fitting we assumed x = 0.012 which is well within the limits of concentration for a boule with a nominal concentration of 0.01. The calculated value for Curie-Weiss temperature is θ_0 = 816 K, in excellent agreement with the data of Spalek et al. [19] which obtained θ_0= -739 ± 47 K

Furthermore, our calculation shows that the next nearest-neighbor Heisenberg interaction energy$|J_2/k_B|$ for zinc compound is of the order of 0.3K which is in excellent agreement with Keesoms experimental results [22].

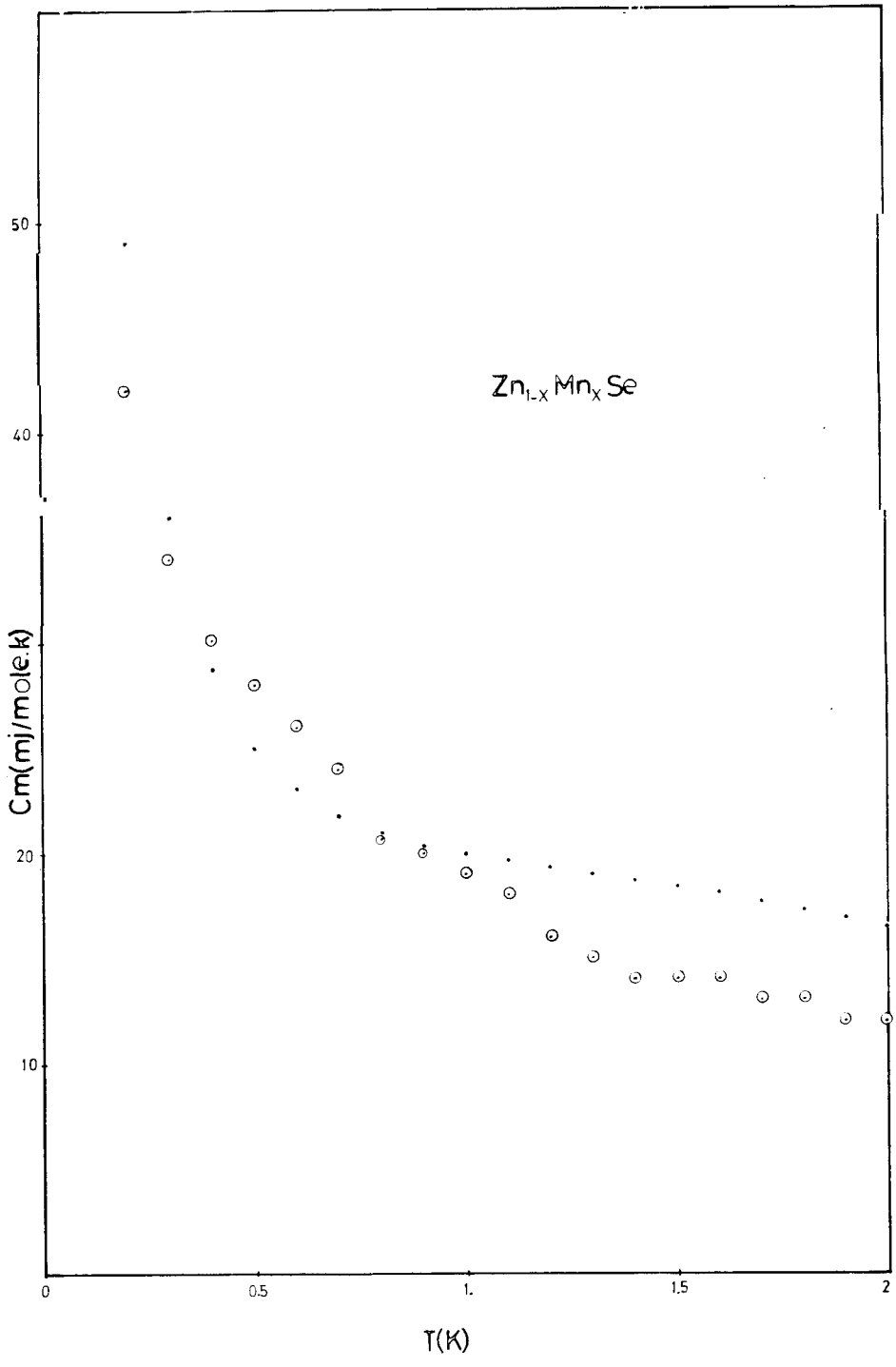

Fig.4. (Θ) Magnetic specific heat of $Zn_{1-X}Mn_XSe$ for x=0.01 as reported by Keesom [22] (based on low temp. specific heat measurements). (.) represents calculation based on the model using X=O.0085, J_1/k_B = -12 .2 K, J_2/k_B = -O.3 k and $J/k_B = -0.7/(R)^{6.8}$ k.

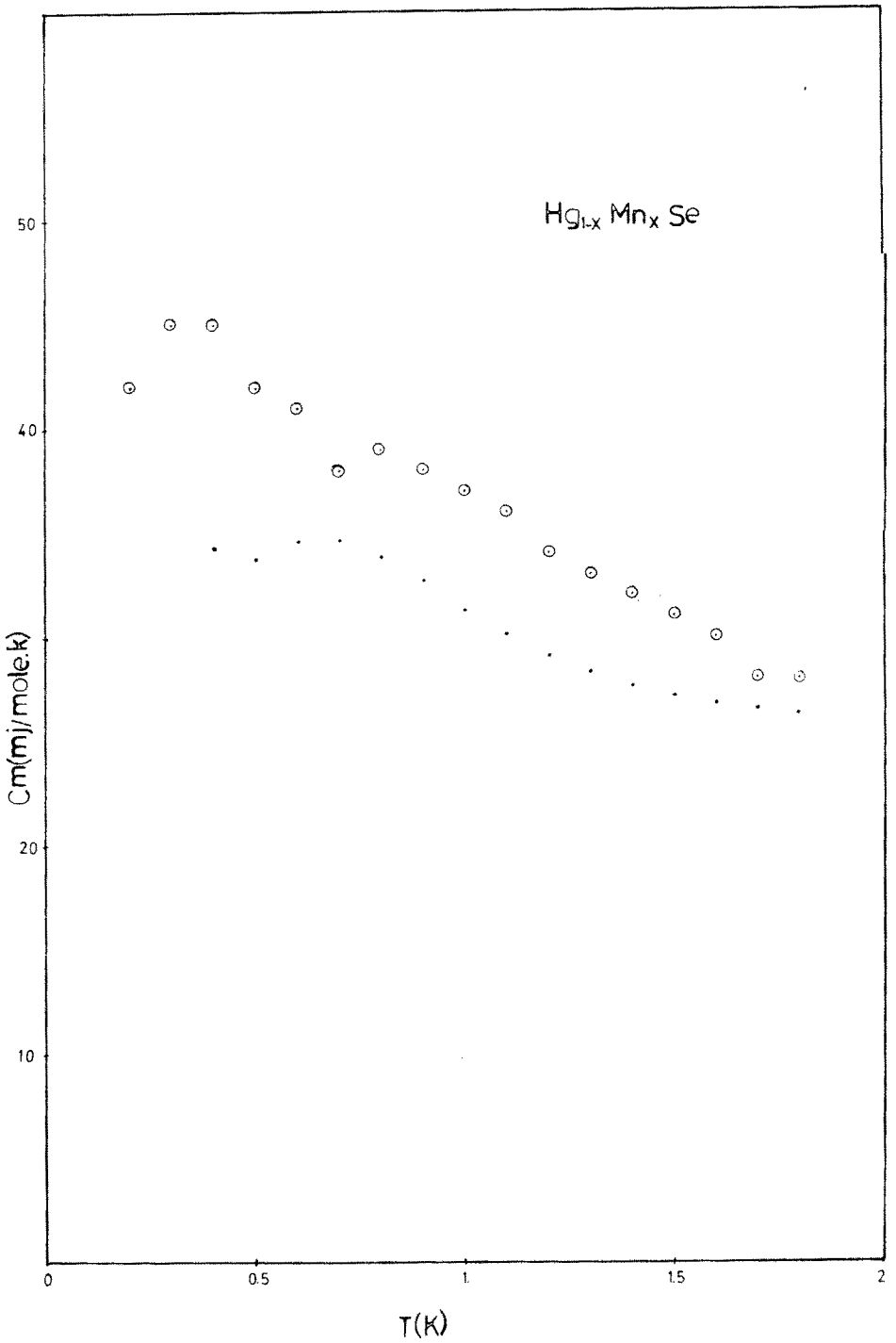

Fig.5. (.) Magnetic specific heat of $Hg_{1-x}Mn_xSe$ for X=0.01 according to Keesom[23] (based on low temp. specific heat measurements). (Θ) represents calculation based on the model using x=O.O12, J_1/k_B= -11.O K, J_2/k_B= -1.1 K and J/k_B=- O.4/$(R)^4$ K.

Table III
Values of nearest -neighbor exchange integral J_1

Material	J_1/k_B	Ref.
Zn_1-xMn xSe	-12.2+0.3	14
Hg_1-xMn xSe	-10.9+0.7	19*

* The real value of interaction is a little less (refer to ref.)

Concluding Remarks

We conclude with two remarks. In our simplified model, clusters with more than two members are ignored. Hence, it would be desirable specially for higher concentrations to extend the present analysis by taking into account the role of larger clusters such as triplets...

Furthermore, in order to complete the present investigation the specific heat data obtained in non-zero external magnetic field should also be compared with calculated results.

Acknowledgements

I wish to express my sincere thanks to Prof. P.H. Keesom for his guidance and encouragement throughout this work. It has also been a pleasure to have had the cooperation and considerable help of Dr. S.M. Amini and Mr. R. Fakhre-Hosseini in the computer calculations.

Finally, the financial support of the Isfahan University of Technology is acknowledged.

References

1. J.K. Furdyna, *J. Appi. Phys.* **53**, 7637 (1982).
2. J.A. Gaj, *J. Phys. Soc. Japan*, **49**, Suppl. A. 797 (1980).
3. J.K. Furdyna, *J. Appl. Phys.* **64**, R29 (1988).
4. E. O. D. U. Bartholomew, et al. *Phys. Rev. B* **38**, (1988)
5. F. F. Geyer and H. Y. Fan, IEEE J. Quantum Electron. QE -16, 1365 (1980)
6. R. R. Galazka et al. *Phys. Rev.* B**22**, 3344 (1980).
S. B. Oseroff, *Phys. Rev.* B**25**, 6584 (1982).
7. S. P. Mc Alister et al. *Phys. Rev.* B **29**, 1310 (1984)
8. S. Oseroff and P. H. Keesom, Semiconductors and Semimetals, Vol. **25**, 1988, Academic Press, Inc.
9. C. J. M. Denissen et al. *Phys. Rev.* B **36**, 5316 (1987).
10. C. J. M. Denissen et al. *Phys. Rev.* B **33**, 7637 (1986).
11. S. Nagata et al. *Phys . Rev.* B **22**, 3331 (1980).
12. M. Jaczynski, et al. *Phys Stat.* Sol. (b), **88**, 73 (1978).
13. M. A. Novak, et al. *J. Appl. Phys.* **57**, 3418 (1985).
14. S. Foner, et al. *Phys. Rev.* B **39**, 11793 (1989).
15. B. E. Larson, et al. *Phys. Rev.* B **33**, 1789 (1986).
16. A. Twardowski, et al. *Phys. Rev.* B**36**, 7013 (1987).
17. K. Matho, *J. Low Temp. Phys.* **35**, 165 (1979)
18. M. Escorne, et al. *Physica* **107 B**, 309 (1981).
19. J. Spalek, et al. *Phys. Rev.* B **33**, 3407 (1986).
20. J. K. Furdina, et al. *Phys. Rev.* B**37**, 3707 (1988).
21. Si. Oseroff, et al. *Phys. Rev.* B**25**, 6584 (1982).
22. P. H. Keesom Phys. *Rev. B***33**, 6512 (1986).
23. P. H. Keesom (private communication)